LYSOSOMAL CAPTURING OF CYTOPLASMIC INJECTED NANOPARTICLES BY AUTOPHAGY: AN ADDITIONAL BARRIER TO NON VIRAL GENE DELIVERY

Katrien Remaut[1], Viola Oorschot[2], Kevin Braeckmans[1], Judith Klumperman[2] and Stefaan C. De Smedt[1]

[1]*Lab General Biochemistry & Physical Pharmacy, Faculty of Pharmaceutical Sciences, Ghent University, Ghent, Belgium,* [2]*Dept. of Cell Biology, Center for Molecular Medicin, Universital Medical Center Utrecht, The Netherlands*

Running head: autophagy on cytoplasmic nanoparticles

Mailing address: Prof. Stefaan De Smedt

Laboratory of General Biochemistry and Physical Pharmacy

Ghent University

Harelbekestraat 72

9000 Ghent-Belgium

Tel.: 0032-9-2648076

Fax.: 0032-9-2648189

E-mail: stefaan.desmedt@ugent.be

ABSTRACT

Autophagy or ‘self-eating’ is a process by which defective organelles and foreign material can be cleared from the cell’s cytoplasm and delivered to the lysosomes in which degradation occurs. It remains an open question, however, whether nanoparticles that did *not* enter the cell through endocytosis can also be captured from the cytoplasm by autophagy. We demonstrate that nanoparticles that are introduced directly in the cytoplasm of the cells by microinjection, can trigger an autophagy response. Moreover, both polystyrene beads and plasmid DNA containing poly-ethylene-imine complexes colocalize with autophagosomes and lysosomes, as was confirmed by electron microscopy. This indicates that cytoplasmic capturing of nanoparticles can occur by an autophagy response. The capturing of nanoparticles from the cytoplasm most likely limits the time frame in which efficient nucleic acid delivery can be obtained. Hence, autophagy forms an additional barrier to non-viral gene delivery, a notion that was not often taken into account before. Furthermore, these findings urges us to reconsider the idea that a single endosomal escape event is sufficient to have the long-lasting presence of nanoparticles in the cytoplasm of the cells.

keywords: cytoplasm, autophagy, microinjection, non-viral gene delivery, CLEM

INTRODUCTION

In non-viral gene delivery, we aim to induce protein production by the cellular administration of plasmid DNA (pDNA) or mRNA that encodes the desired protein (Fig 1). For gene therapy to be successful, the nucleic acids should reach the cytoplasm (in the case of mRNA) or the nucleus (in the case of pDNA) of the target cells. The ideal delivery system should guide the nucleic acids to their target cells, increase their cellular uptake and help the nucleic acids to escape from the endosomal compartment into the cytoplasm of the cells. Also, the possible degradation of the nucleic acids in the intracellular environment should be taken into account, as the intact sequence is necessary to maintain their biological activity (1).

Since more than a decade, pharmacists, material scientists and biophysicists are intensively studying the design, preparation and cell biological behavior of nanosized particles carrying nucleic acids (2-9). The extensive research of nucleic acids delivery has revealed some general findings which should be taken into account when developing new gene delivery systems. It is for example accepted that positively charged nanoparticles are better taken up by cells (10). As naked nucleic acids are negatively charged, they are complexed with cationic polymers or cationic liposomes to increase the cellular delivery. These complexes can take different endocytic pathways to enter the cells, dependent on their size and surface characteristics (11-14). When nanoparticles fail to escape the endosomal compartment, eventual delivery to (and degradation in) the lysosomes will occur. Up to now, it is accepted that nanoparticles or naked nucleic acids that escaped from the endosomal compartment remain present inside the cytoplasm of the cells. We recently obtained evidence, however, that nanoparticles that are freely present inside the cytoplasm, can be captured inside cellular vesicles, possibly due to an autophagic response of the cells (15). Autophagy or ‘self-eating’ is a process by which cells clear their cytoplasm from defective cell organelles and foreign material (Fig 1) (16). Initially, part of the cytoplasm is engulfed by a double-membraned structure (the phagophore, Fig 1, step 7), which closes on itself to form an autophagosome (Fig 1, step 8). These autophagosomes can receive additional input from endocytic vesicles before they eventually fuse with lysosomes to form an autolysosome, in which the sequestered cytoplasmic cargo is degraded (Fig 1, step 9). Recently, it was

shown for the first time that autophagy is a potential barrier in non-viral gene delivery after transfection of cells with nanoparticles. With electroporation, however, an autophagy response was not noted (17). Also previously, we suggested that autophagy could be responsible for the long term endosomal entrapment of nanoparticles in Retinal Pigment Epithelial (RPE) cells (18). In the current paper, we demonstrate the occurrence of autophagy on inert polystyrene beads and plasmid DNA containing poly-ethylene-imine (PEI) nanoparticles, that were directly introduced in the cytoplasm of the cells by microinjection (Fig 1, 10). Our findings suggest that, highly likely, endosomal escape alone is not sufficient to prevent cargo from eventual lysosomal degradation. The re-capturing of cytoplasmic nanoparticles in autophagosomes will limit the residence time of cytoplasmic cargo and could be a major determinant of why the majority of nanoparticles are entrapped in the endosomal compartment. This on its turn limits the time frame during which mRNA can be translated in the cytoplasm, or pDNA can be delivered to the nucleus of the cells, thus limiting the efficiency of non-viral gene delivery systems.

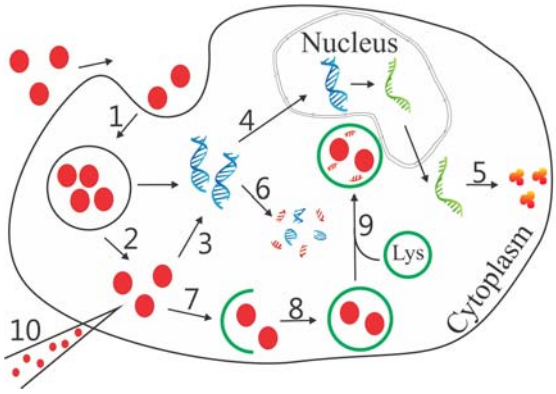

Fig1. Intracellular barriers to non-viral gene delivery. After cellular entry (1), nanoparticles have to escape from the endosomes (2) and release nucleic acids in the cytoplasm of the cells (3). Plasmid DNA then needs to travel to the nucleus (4), while mRNA can be translated to proteins in the cytoplasm of the cells (5). Clearly, degradation of nucleic acids should be avoided (6). When autophagy occurs, a phagophore isolates cytoplasmic material (7) and closes on itself to form an autophagosome (8). These fuse with lysosomes to form an autolysosome (9) in which the cytoplasmic cargo is degraded. In this research article, nanoparticles are directly delivered to the cytoplasm of the cells by microinjection (10).

MATERIALS AND METHODS

1. pDNA production & labeling

Heat competent *E. coli* transformed with the gWIZ-GFP plasmid DNA (GeneTherapy Systems®, San Diego, California) were grown in LB medium with kanamycin at 37 °C for 20 h. pDNA was isolated and purified with the Qiafilter Plasmid Giga Kit (Qiagen®, Venlo, The Netherlands) according to the manufacturer's instructions. For colocalization experiments, pDNA was labeled with Cy5 (fluorescent red) using the *Label* IT® Cy™5 labeling kit (Mirus Bio Corporation, WI, USA) and purified by purification columns as supplied by the manufacturer. It should be noted that at the highest labeling density used, the Cy5-labeled pDNA can no longer induce GFP expression so it does not interfere with the colocalization measurements (19).

2. Polystyrene beads and pDNA/PEI polyplexes

Green fluorescent carboxylated polystyrene beads of 100 nm and red fluorescent carboxylated polystyrene beads of 40 nm were used (Molecular Probes®). These beads have a negative ζ-potential and were introduced into the cells by microinjection, uptake or electroporation as described below. As working solution, polystyrene beads were freshly diluted 1000 times in water and sonicated during 15 minutes before use. The diluted PS beads have an average concentration of 2 x 10^8 beads/µl. Upon injection, this results in between 8 to 20 injected beads per cell.

As pDNA nanoparticles we made use of pDNA complexed to 22 kDa linear poly-ethylene-imine (PEI) (kindly provided to us by Prof. Olivia Merkel, Wayne State University, USA). Complexes were prepared by adding a PEI polymer solution to an equal volume of a 0.4 µg/µl pDNA solution to obtain a nitrogen to phosphate ratio (N/P ratio) of 10, followed by vortexing the dispersion for 10 seconds. pDNA/PEI complexes were allowed to equilibrate at room temperature for 30 minutes prior to use. pDNA/PEI complexes have a positive zetapotential of 32 ± 5 mV and a size of 165 ± 15 nm in Hepes buffer. It should be noted that both for polystyrene beads and pDNA/PEI nanoparticles, the size and charge can change significantly in cell culture medium or optiMEM® (20).

For microinjection, 2 µl of beads (1000x diluted) or pDNA/PEI complexes were added to 6 µl of water or 1 µl 70 kDa TRITC-dextran and 5 µl of water. These solutions were filtered over a 450 nm filter (Millipore™, Overijse, Belgium) to avoid clogging of the microinjection needles. For electroporation, 10 µl of diluted beads or pDNA/PEI complexes were added to the cell in optiMEM®. For uptake experiments, 5 µl of diluted beads or pDNA/PEI complexes were incubated in cell culture medium for 2 hours at 37°C.

3. Cell culture conditions

HeLa cells (human epithelial cervical carcinoma cells, ATCC CCL-2, France) or HeLa cells stably expressing GFP-LC3 (kindly supplied to us by Prof. Felix Randow, Cambridge, UK) were cultured in phenol red free DMEM-F12 (Gibco-Invitrogen, Merelbeke, Belgium) containing 2 mM glutamine, 10% heat-inactivated fetal bovine serum (FBS) (Hyclone/Perbio, Thermo Fisher Scientific, Erembodegem-Aalst, Belgium) and 100 U/ml penicillin-streptomycin (Invitrogen-Gibco, Merelbeke, Belgium) at 37 °C in a humidified atmosphere containing 5% CO_2. HeLa cells were seeded in 35 mm glass bottom culture dishes (MatTek Corporation®) the day before use. For electron microscopy gridded coverslips were used, coated with Formvar and Gelatin as described before (21).

4. Microinjection

Microinjection with the polystyrene beads (green or red) or Cy5-pDNA/PEI nanoparticles (red) was performed with a Femtojet® microinjector and an Injectman® NI 2 micromanipulator (Eppendorf®) installed on a Nikon EZC1-si confocal laser scanning microscope. Injection needles were pulled from borosilicate glass capillaries (1.2 mm outer diameter and 0.94 mm inner diameter) with a P-1000 flaming/brown micropipette puller (Sutter Instruments, California, USA). Injections were performed in the cytoplasm, using polystyrene beads or pDNA/PEI complexes in HEPES buffer. If needed, injection solutions were supplemented with 2 mg/ml 70 kDa TRITC-dextran (Sigma-Aldrich®) to identify the place of injection. Typically, about 30-50 successful injections were performed during a 20 minutes time period. After microinjection, cells were incubated for an additional 24 hours before taking fluorescence microscopy images. Labeling of the lysosomes was performed by transfecting the

cells with CellLight™ Lysosomes-GFP BacMam 2.0, following the manufacturer's instructions (Invitrogen®). Colocalization with LC3 was evaluated using HeLa cells stably expressing GFP-LC3. The basal expression levels of non-injected cells expressing GFP-LAMP1 and GFP-LC3 can be found in supplementary information (Suppl. Fig. 1). For live-cell imaging, the cells were placed on the microscope in a stage top incubation chamber (Tokai Hit, Shizuoka, Japan), set at 37 °C, 5% CO2, and 100% humidity. Live-cell single particle tracking was performed on a custom-built laser widefield fluorescence microscope setup (TE2000-E inverted microscope) equipped with a Plan Apo VC 100x 1.4 NA oil immersion objective lens (Nikon Belux, Brussels, Belgium). Videos were acquired in NIS Elements (Nikon Benelux, Brussels, Belgium) at a frame speed of 30 frames per second and exposure times between 10 and 30 ms.

5. Electroporation and uptake

1.2 x 10^6 HeLa cells were electroporated at 260 V and 850 µF in 400 µl optiMEM containing the 100 nm green polystyrene beads. Then, cells were centrifuged and washed with PBS to remove remaining nanoparticles from the culture medium. Cells were resuspended in culture medium and seeded in 35 mm glass bottom culture dishes. After 24 hours, cells were fixed in 4% paraformaldehyde and prepared for electron microscopy as described below. For uptake experiments, nanoparticles were incubated with HeLa cells during 2 hours at 37°C in culture medium. Then, cells were washed 3 times with PBS and incubated for an additional 24 hours in culture medium.

6. Correlative light electron microscopy (CLEM)

Hela cells were grown at 20 % confluency on gridded glass coverslips and micro-injected with 100 nm green polystyrene beads. A DIC map of the injected cell was recorded to mark the position on the coverslip. After 24 hours incubation cells were fixed by adding freshly prepared 4% formaldehyde in 0.1 M phosphate buffer pH 7.4 to an equal volume of culture medium for 10 min, followed by post-fixation in 4% formaldehyde in 0.1 M phosphate buffer pH 7.4. Cells were stored until further processing in 1% formaldehyde at 4˚C. Processing of cells for embedding was done as described (21).

Briefly, wash the fixed cells on coverslips with 0.05 M glycine in PBS. Mount the coverslip onto a glass slide using Mowiol. Locate the region of interest by using the DIC map and mark this region with a nailpolish dot on the backside of the coverslip. Remove the coverslip from the glass slide by immersing it in PBS. Place the coverslip with cells facing up in a 3 cm Petri dish and rinse with PBS containing 0.1% BSA to facilitate gelatin spreading. Incubate the coverslip with 800 µl 6% gelatin in PBS for 30–60 min in a wet chamber at 37 °C. This allows the gelatin to disperse in between the cell layer. Rinse the coverslip with PBS containing 0.1% BSA, remove all the PBS/BSA and add 400 µl 12% gelatin with erythrocytes at 37 °C. Allow to solidify for 30 min at 4 °C. Fix the sample for 30 min with 0.5% paraformaldehyde in PBS at 4 °C and rinse twice with cold PBS. Incubate the coverslip for 30 min with cold 2.3 M sucrose. Then replace the solution in the dish with fresh sucrose solution, and place the dish for 3 days on a rocker at 4 °C to allow infusion of sucrose into the gelatin and cell layer. Use a razor blade to cut out a small (2–3 mm) block containing the region of interest. Mount the block on a specimen holder (pin) with the erythrocyte layer facing the specimen holder. Freeze in liquid nitrogen.

Ultrathin cryosectioning was done on a Leica Ultracut cryotome (UC6/FC6). To pick up ultrathin (65 nm) cryosections a 1:1 mixture of 2.3 M sucrose and 1.8% methylcellulose was used. Sections were placed on cupper grids, which contained a formvar film and were carbon coated. Labeling principles are described (22). Correlative microscopy of fluorescence- and immunogold-labeled ultrathin cryosections was done essentially as described (23) with a few adaptations. Briefly, grids were incubated on 2% gelatin in PBS for 20 min at 37˚C, then incubated with mouse anti-human Lamp 1 CD107a (BD Pharmingen 555798) in 1% BSA in PBS for 45 min, rinsed in 0.1% BSA in PBS, incubated with rabbit anti mouse IG (Dako Z0412) for 30 min., rinsed in 0.1% BSA in PBS and incubated with goat anti-rabbit Alexa 488-conjugated antibodies (Molecular Probes) for 45 min. Grids were rinsed followed by incubation with protein A conjugated to 10 nanometer gold particles (Department of Cell Biology, UMC, Utrecht) for 20 min, fixed for 5 min with 1% glutaraldehyde in PBS, rinsed in PBS and incubated in Hoechst 33342 (1 mg/ml) in PBS. For fluorescence, grids were mounted between a microscope slide and coverslip with 50% glycerol and imaged in a Deltavision RT microscope (Applied Precision, Issaquah WA) using an EMCCD camera. For subsequent transmission

electron microscopy, grids were unmounted, washed in water, incubated for 5 min in 2% uranyl acetate and 0.15 M oxalic acid and subsequently for 5 min in 0.4% uranyl acetate and 1.8% 25ctp methylcellulose. Grids were viewed in a JEOL 1010 or in a Tecnai 12 (FEI) electron microscope. The classification of vesicles as early endosomes, late endosomes or lysosomes was done based on the morphological appearance of the vesicles in the EM images, combined with anti-LAMP1 staining, which only labels late endosomes and lysosomes (24).

7. Single Particle Tracking and Colocalization analysis

Single Particle tracking was performed on about 10 cells per time point. For each cell, typically 5 to 10 movies of about 200 frames were recorded. Using an in-house developed software, a distribution of alpha values was obtained, giving information on the mode of transport. Nanoparticles with an alpha value of < 0.4 were considered immobile. Nanoparticles with an alpha value > 1 are showing directed transport. Nanoparticles with alpha values between 0.4 and 1 mostly resulted from tracks showing directed transport during part of the track, in combination with a stationary phase in the same track. For a more detailed description of both the SPT microscope and the trajectory analysis, the reader is referred to (18). For confocal images, colocalization analysis of red fluorescent nanoparticles with the green labeled cellular compartments were performed in Image J, using two different colocalization plugins (colocalization and the JACOp plugin) (25) (http://rsbweb.nih.gov/ij/). To avoid false positive correlation between diffuse fluorescence in the green channel with nanoparticles in the red channel, object based colocalization was performed to determine the percentage of colocalized nanoparticles.

RESULTS

Previously, we explored the possibility of chromatin targeting to increase the delivery of nanoparticles to the nucleus of the cells (15). In the *in vitro* Xenopus nuclear envelope reassembly reaction, chromatin targeting could be improved up to 3-fold. We noted, however, that upon microinjection of these nanoparticles in the cytoplasm of the cells, nanoparticles were not able to reach the nucleus of the cells during cell division. It seemed, however, that nanoparticles accumulated in a specific perinuclear region, where also lysosomes are abundant. We hypothesized that this cytoplasmic capturing of nanoparticles was responsible for the lack of chromatin targeting in living cells. In this research project, we were interested to evaluate if nanoparticles that are present in the cytoplasm of the cells, could indeed be captured inside lysosomal vesicles due to the occurrence of autophagy. Therefore, we investigated the fate of injected polystyrene beads and pDNA/PEI nanoparticles with a combination of Single Particle Tracking (SPT), fluorescence colocalization microscopy and electron microscopy.

1. Single color single particle tracking (SPT)

To reach the nucleus of the cells, nanoparticles should show some mobility in the cytoplasm of the cells. In a first set of experiments, we injected 100 nm green polystyrene beads in the cytoplasm of the cells and followed their mobility using Single Particle Tracking (SPT). Figure 2 shows the movement of 100 nm green polystyrene beads after injection into the cytoplasm of the cells. Immediately after injection, 100 nm beads are completely immobile in the cytoplasm of the cells. Tracks of individual beads remain stationary at a single spot (Fig 2B). Even upon close view on individual tracks (Fig 2C), no diffusion can be seen in the time course of the movies. Analysis of more than 1000 tracks revealed that 89 ± 4 percent of the nanoparticles have an alpha value of less than 0.4, demonstrating restricted motion (Fig 2H, black bars). This indicates that the nanoparticles are too large to travel through the cytoplasm of the cells, or, more likely, that the charged beads get stuck after binding to oppositely charged intracellular compartments. It should be noted that nanoparticles appear to be present in the

nucleus of the cells. However, as we use a wide-field confocal set up to acquire the movies, these beads are most likely present above or below the nucleus, and not actually in the nucleoplasm.

Next, injected cells were incubated overnight at 37 °C. When the injected cells where viewed with SPT after this time period, movement of the injected beads was clearly observed. When compared to the beads immediately after injection, the particles show longer tracks and directed motion (Fig 2F). This is also obvious by a shift of the alpha value towards larger values (Fig 2G, grey bars). 59 ± 6 percent of nanoparticles move with alpha values between 0.4 – 1, while even 19 ± 7% have an alpha value of more than 1, indicating directed motion (Fig 2H, grey bars). This directed motion can be clearly distinguished from Brownian diffusion and typically occurs when nanoparticles are transported inside endosomal/lysosomal vesicles, along the microtubuli. The increased mobility and active transport of nanoparticles upon incubation of the injected cells suggests that the initially immobile cytoplasmic nanoparticles are now present in endocytic vesicles, as would occur upon autophagy.

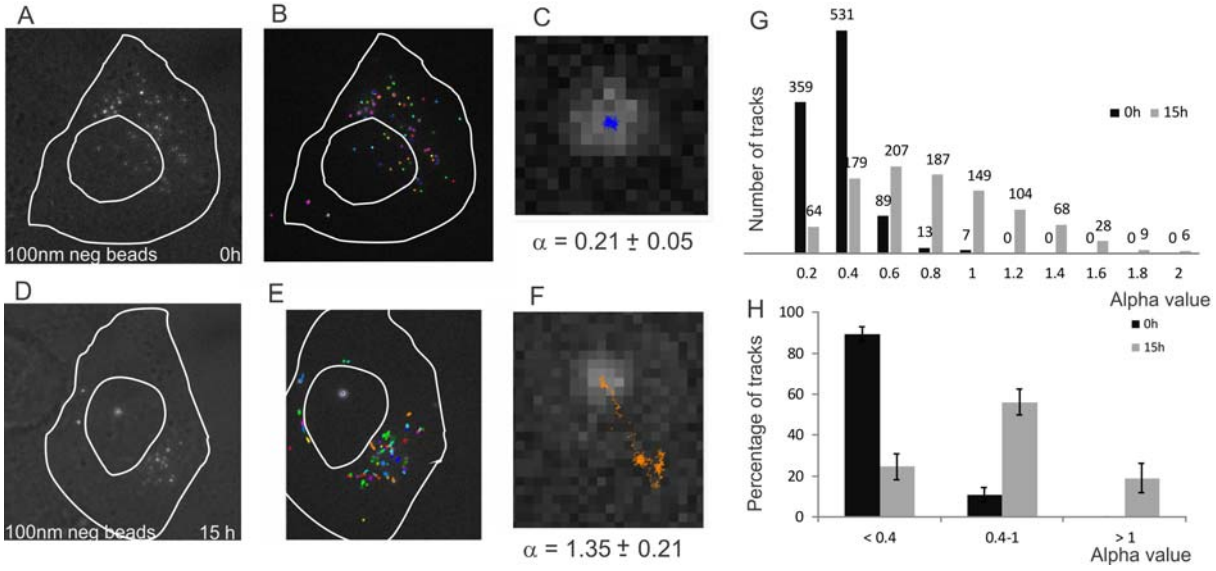

Fig2. Single particle tracking in HeLa cells injected with 100 nm negatively charged green polystyrene beads. (A and D) Transmission image immediately and 15 hours following injection, (B and E) tracks of polystyrene beads and (C and F) zoom in on a single track. The position of the cytoplasm and nucleus is demonstrated by white lines. (G) represents a histogram of the number of tracks with an alpha value as depicted in the x-axis. (H) shows the percentages of tracks with an alpha value as depicted in the x-axis. Black bars: immediately after injection. Grey bars: after overnight incubation. Representative videos can be viewed in supplementary information.

2. Colocalization of nanoparticles with lysosomes and autophagosomes

When autophagy occurs, nanoparticles will eventually be delivered to the lysosomal compartment. We demonstrated previously, that immediately after injection, there is no colocalization of the nanoparticles with endosomes or lysosomes, which is expected as the nanoparticles are not taken up by the cells by endocytosis, but are directly delivered to the cytoplasm (15). To verify whether injected nanoparticles reach lysosomes, we injected HeLa cells expressing GFP-LAMP1 (a lysosomal marker) with red labeled polystyrene beads or pDNA/PEI nanoparticles and determined the colocalization with the lysosomes 24 hours after injection. Figure 3 demonstrates that both red polystyrene beads and pDNA/PEI complexes colocalize with GFP-LAMP1 positive lysosomes, as indicated by the white spots in figure 3C. The insert in figure 3 clearly demonstrates a GFP-LAMP1 positive lysosomal membrane that surrounds a pDNA/PEI particle, giving additional prove that the injected nanoparticles are now present inside lysosomes, and not just accidentally present in the same intracellular region. This finding indicates that autophagy could occur on the injected nanoparticles. Colocalization analysis demonstrates that 77 ± 9 % of polystyrene beads and 74 ± 7 % of PEI/DNA nanoparticles colocalizes with GFP-LAMP1 positive vesicles (Fig 6).

A first step in autophagy, is the sequestration of cytoplasmic cargo by a phagophore. This phagophore than closes to form a double-membraned structure, named the autophagosome (16). The presence of autophagosomes can be determined by “microtubule-associated protein 1A/1B light chain 3” (LC-3) staining (26). Therefore, HeLa cells expressing GFP-LC3 (green) were injected with red labeled nanoparticles and the colocalization between the nanoparticles and autophagosomes was assessed 24 hours after injection. Figure 4 shows that both polystyrene beads and pDNA/PEI nanoparticles colocalize with the autophagosomes, indicating that autophagy does indeed occur on these injected nanoparticles. It should be noted that there are still nanoparticles (red in Fig 4, colocalization) that do not colocalize with GFP-LC3, indicating that these nanoparticles are still freely present in the cytoplasm of the cells. Alternatively, autophagosomes carrying these nanoparticles could already have fused with lysosomes. As the inner autophagosomal membrane degrades in the

lysosomes, this results in the loss of the GFP-LC3 signal. Fig. 6 indeed confirms that less nanoparticles are colocalized with GFP-LC3 when compared to GFP-LAMP1.

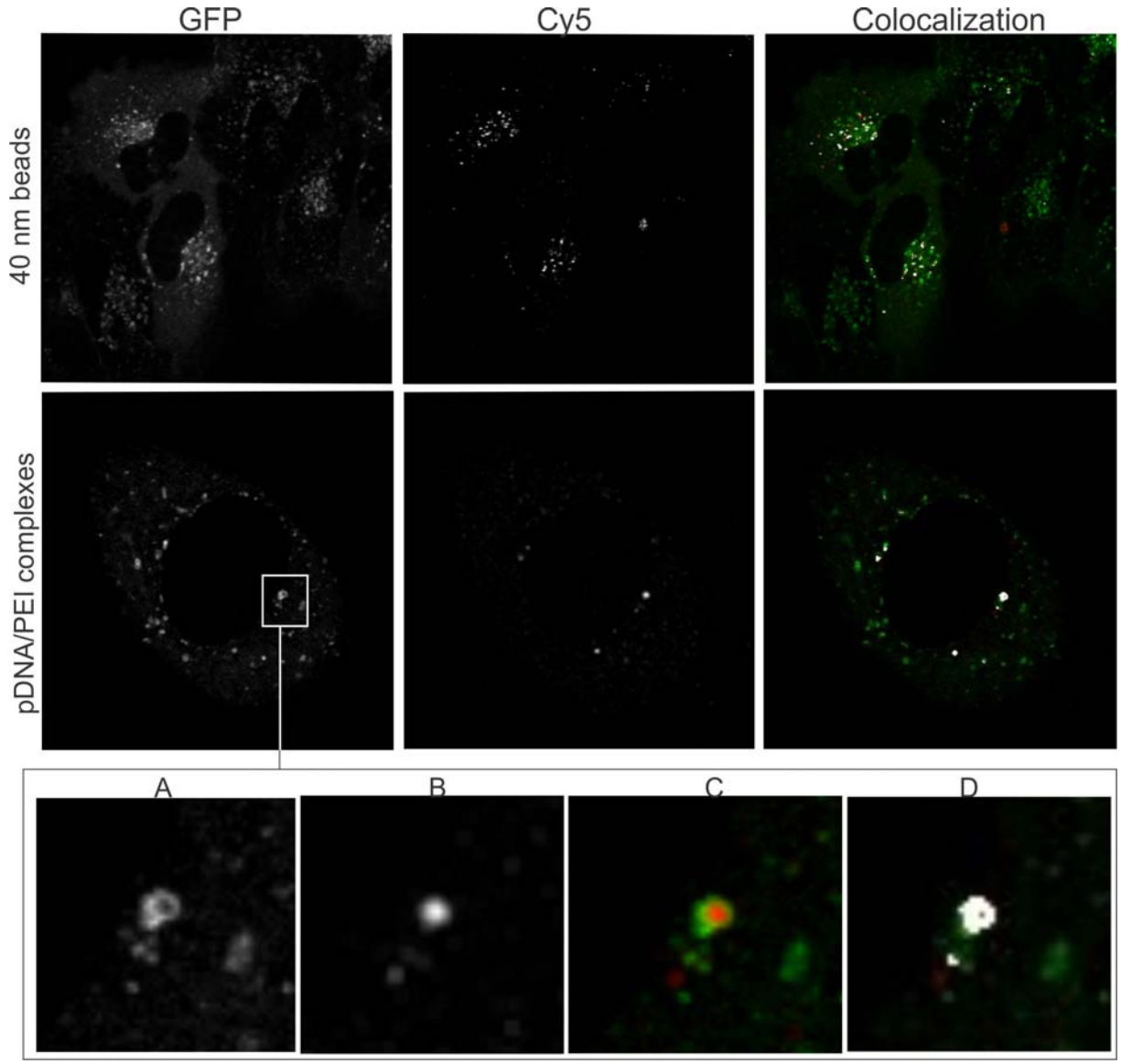

Fig 3. Confocal images of HeLa cells expressing GFP-LAMP1 (GFP), that were injected with red labeled polystyrene beads or pDNA/PEI nanoparticles (Cy5). Colocalization between green and red fluorescence is shown as white dots, while non-colocalized lysosomes or nanoparticles appear in green or red respectively (Colocalization). Insert shows a detail of a GFP-LAMP1 positive membrane (A, green channel) that surrounds a pDNA/PEI nanoparticle (B, red channel). C represent the overlay of A and B, while D depicts the colocalized pixels in white.

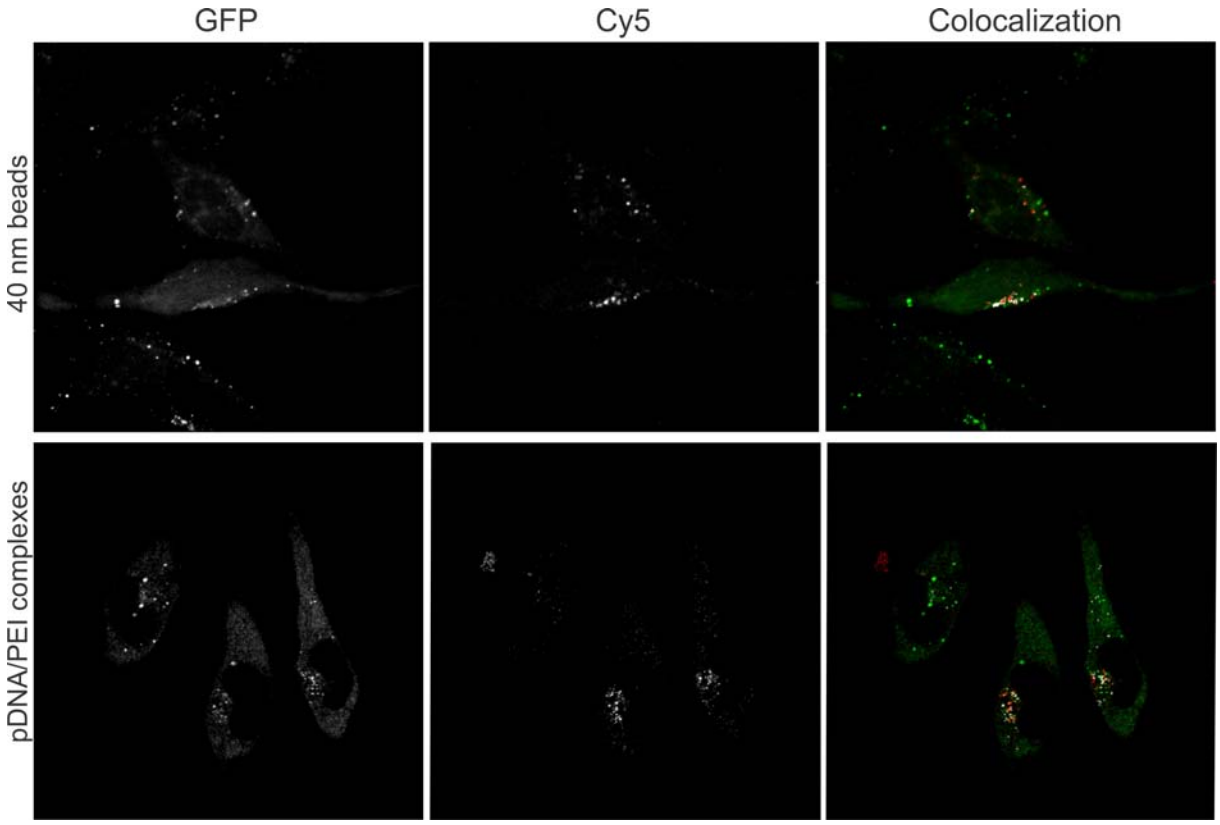

Fig 4. Confocal images of HeLa cells expressing GFP-LC3 (GFP), that were injected with red labeled polystyrene beads or pDNA/PEI nanoparticles (Cy5). Colocalization between green and red fluorescence is shown as white dots, while non-colocalized autophagosomes or nanoparticles appear in green or red respectively (Colocalization).

To evaluate whether autophagy also plays a role in the fate of endocytosed nanoparticles, we next investigated the colocalization with GFP-LC3 of polystyrene beads and pDNA/PEI nanoparticles that were taken up by endocytosis (Figure 5). Also here there is partial colocalization with GFP-LC3, indicating that autophagosomes can receive input from endocytic vesicles, as has been suggested before (16). Alternatively, nanoparticles could first have escaped from the endosomal compartment and subsequently captured in autophagosomes. It should be noted that cells incubated with pDNA/PEI nanoparticles (bottom row) show more and larger GFP-LC3 vesicles, when compared to non-tretaed cells or cells incubated with polystyrene beads (Figure 5, GFP and Suppl. Fig. 1). The increase in the amount and size of GFP-LC3 vesicles is indicative for the upregulation of the autophagy pathway in the cells transfected with pDNA/PEI nanoparticles. It therefore seems likely that pDNA/PEI nanoparticles induce autophagy more when compared to polystyrene beads, which could be attributed

to the presence of foreign pDNA in these complexes (27). The fact that PEI/DNA nanoparticles are taken up significantly more than polystyrene beads in GFP-LC3 positive vesicles, both after injection or when delivered through endocytosis can also be seen from the colocalization analysis presented in Fig. 6.

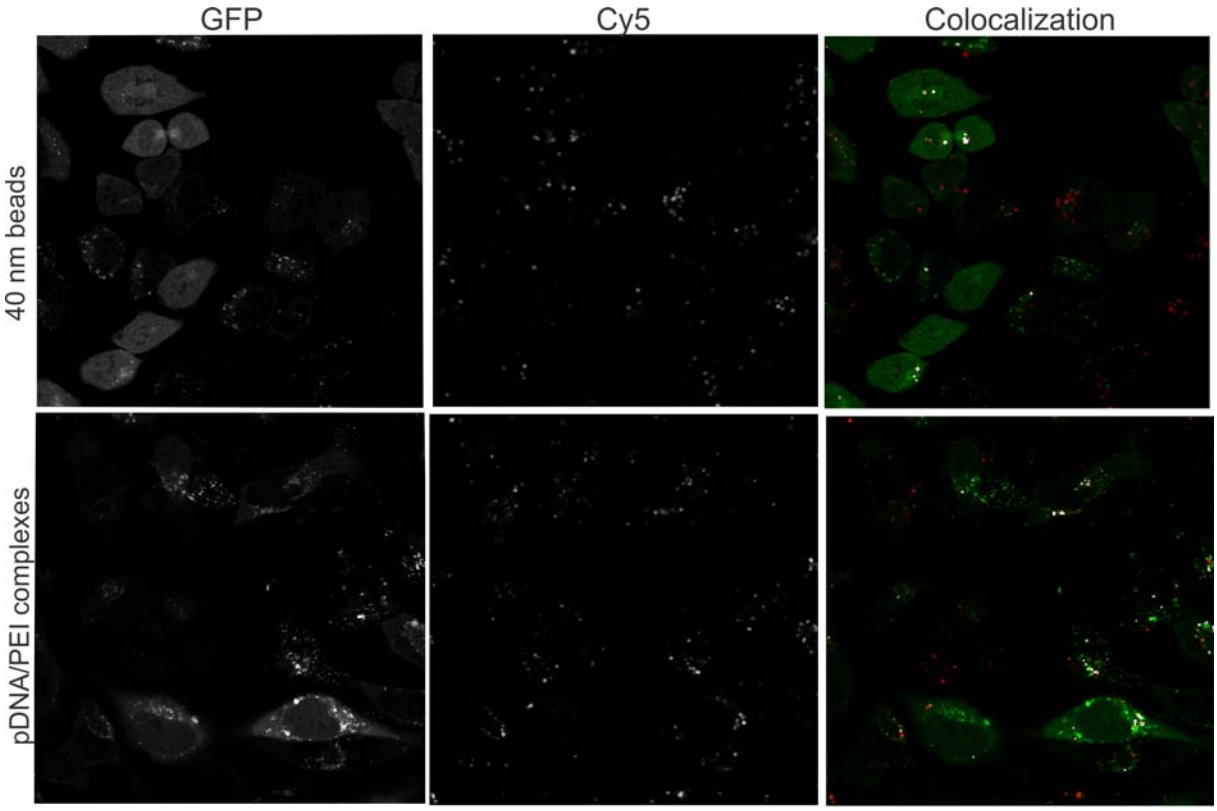

Fig 5. Confocal images of HeLa cells expressing GFP-LC3 (GFP), that were incubated with red labeled polystyrene beads or pDNA/PEI nanoparticles (Cy5). Colocalization between green and red fluorescence is shown as white dots, while non-colocalized autophagosomes or nanoparticles appear in green or red respectively (Colocalization).

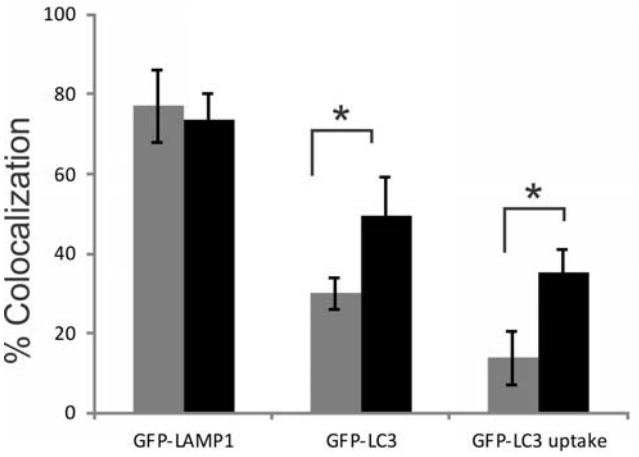

Fig 6. Percentage of colocalization between red polystyrene beads (grey bars) and red PEI/DNA nanoparticles (black bars) with green labeled GFP-LAMP1 or GFP-LC3 vesicles as depicted in the x-axis. (GFP-LC3 uptake) shows colocalization when nanoparticles were taken up by endocytosis. Significant differences between polystyrene beads and PEI/DNA nanoparticles were determined by a student t-test. * denotes a P value < 0.05.

3. Electron microscopy on electroporated or microinjected beads reveals an autophagy response

The above mentioned experiments strongly indicate that microinjected nanoparticles can be trapped from the cytoplasm in autophagosomes, with eventual delivery to the lysosomes. To elucidate if injected nanoparticles were truly present inside lysosomal vesicles, electron microscopy on cryosections of microinjected cells was performed. First, we evaluated if the presence of polystyrene beads in the cells could be distinguished in the EM images. Therefore, cells were incubated with 100 nm or 40 nm polystyrene beads. Figure 7 shows that polystyrene beads can be identified in the early endosomes (EE) as well as later stages of the endosomes (E). Endosomal cross sections could contain between 1 to 10 polystyrene beads of 100 nm and up to 20 – 30 polystyrene beads of 40 nm.

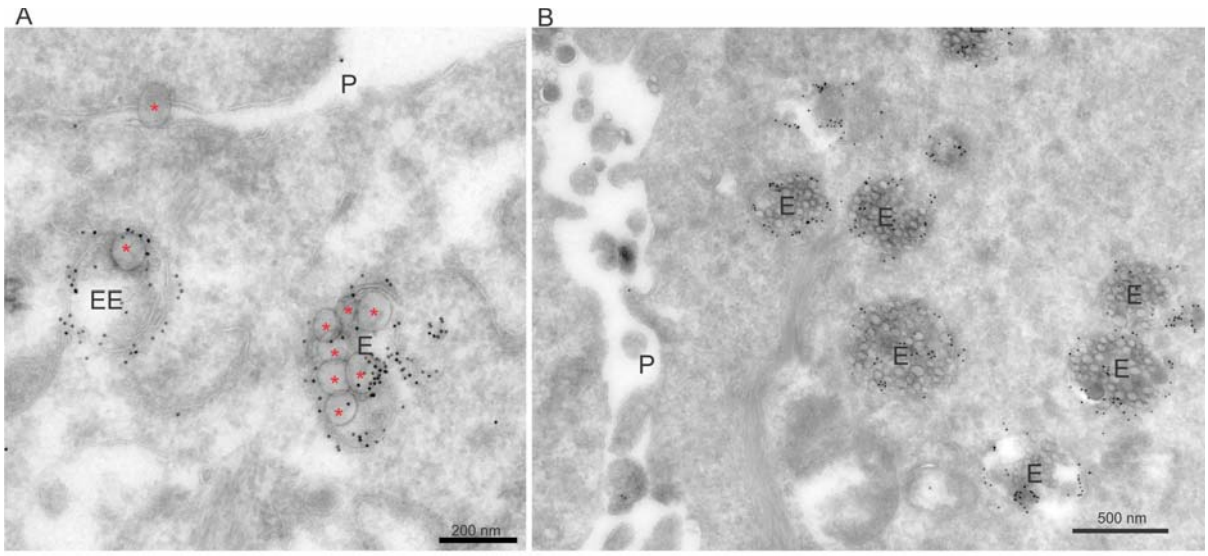

Fig 7. Electron Microscopy of HeLa cells immune gold-labeled for LAMP1 (10 nm gold particles, black dots), that were incubated with 100 nm (A) or 40 nm (B) polystyrene beads. Polystyrene beads (indicated with red asterix in A) are clearly visible in the endosomal lumen. P: plasmamembrane, EE: early endosome, E: later stage endosomes. Cells were fixed and processed 24 hours after the initial administration of nanoparticles.

Next we investigated HeLa cells that were electroporated with 100 nm polystyrene beads. In electroporation, an externally applied electrical field temporarily permeabilizes the plasma membrane, allowing cytoplasmic delivery of free nucleic acids and nanoparticles. Figure 8 shows 3 representative examples of HeLa cells in which nanoparticles were delivered to the cytoplasm after electroporation. We find the polystyrene beads in large vacuoles (endosomes/lysosomes) (Figure 8A – B), with a heterogene content, typical for endo-lysosomal compartments involved in autophagy. In Figure 8C, the vacuoles even contain 2 mitochondria (M). As mitochondria are cytoplasmic organelles, this indicates these endo-lysosomes are autophagic structures that cleared the cytoplasm from defective cell organelles and the polystyrene beads. Together, these images indicate that cytoplasmic beads are indeed cleared from the cytoplasm of cells by an autophagy response.

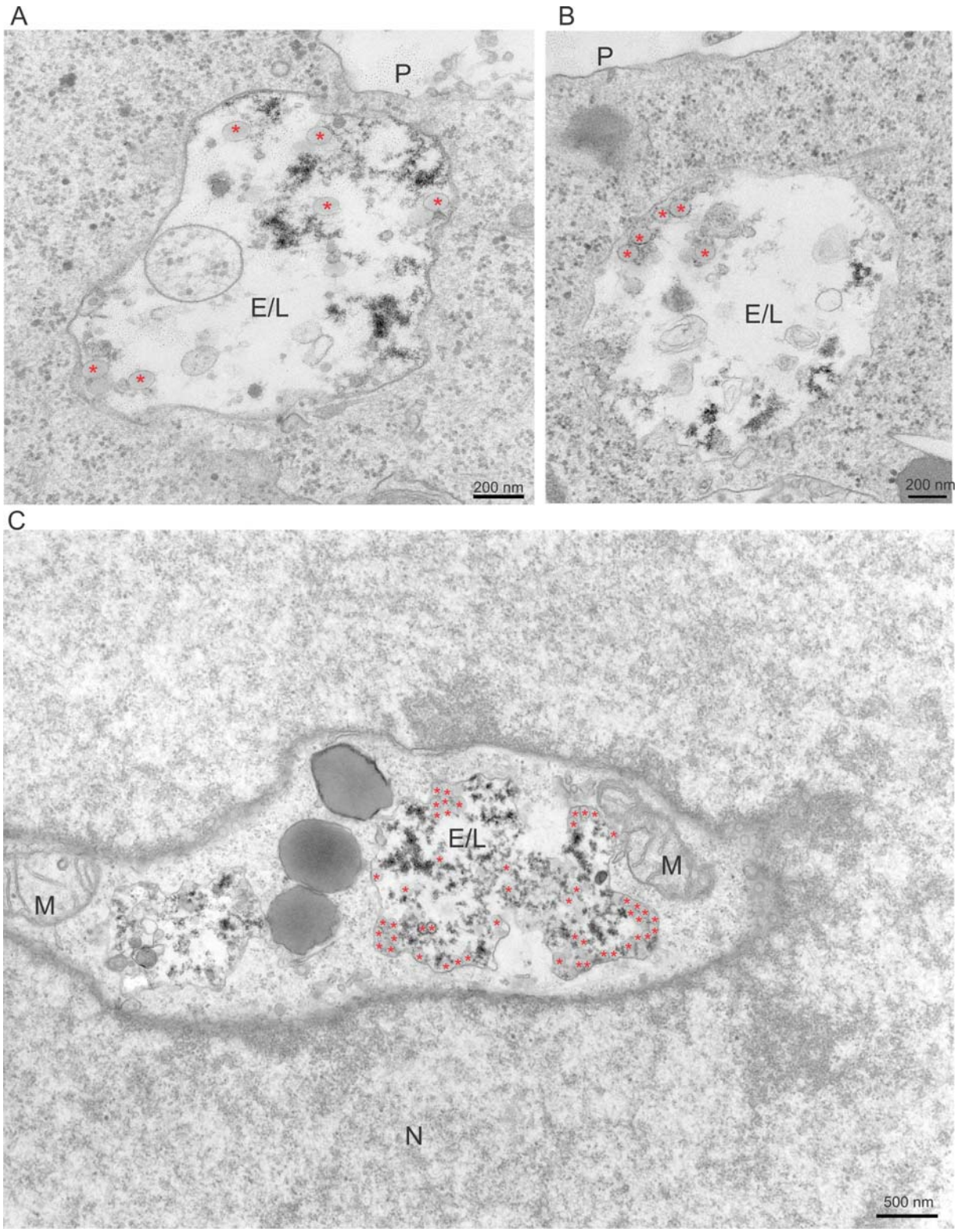

Fig 8. Electron Microscopy of HeLa cells that were electroporated with 100 nm polystyrene beads. Polystyrene beads are indicated with a red asterix. P: plasma membrane, N: nucleus, E/L: endosome/lysosome, M: mitochondrion. Cells were fixed and processed 24 hours after the initial administration of nanoparticles. (A, B and C) represent 3 different cells.

Finally, EM images were taken from HeLa cells that were injected with polystyrene nanoparticles. Therefore, cells of interest were first imaged with fluorescence microscopy to determine their position on the gridded coverslip (for example I_9 in figure 9 A-D). From the selected cells, cryosections were taken which were immune gold-labeled for LAMP1 and the intracellular location of the injected polystyrene beads was determined with EM. Figure 9, E and F demonstrates that injected polystyrene beads can be found inside LAMP1 positive late endosomes/lysosomes, indicating they were indeed captured from the cytoplasm and delivered to these endocytic vesicles. It should be noted that most vesicles contained only 1 polystyrene bead in contrast to beads that were taken up by endocytosis in which up to 10 beads were present in the endocytic vesicles. We cannot rule out the possibility that some injected polystyrene beads are washed away from the cells during the subsequent fixation and washing steps. Alternatively, exocytosis of the injected nanoparticles could already have lowered the intracellular concentration of beads in the cytoplasm of the cells. It should be noted, however, that although finding beads was a rare event, when they were found, they were only present in lysosomal vesicles and never in the cytoplasm or the nucleus of the cells.

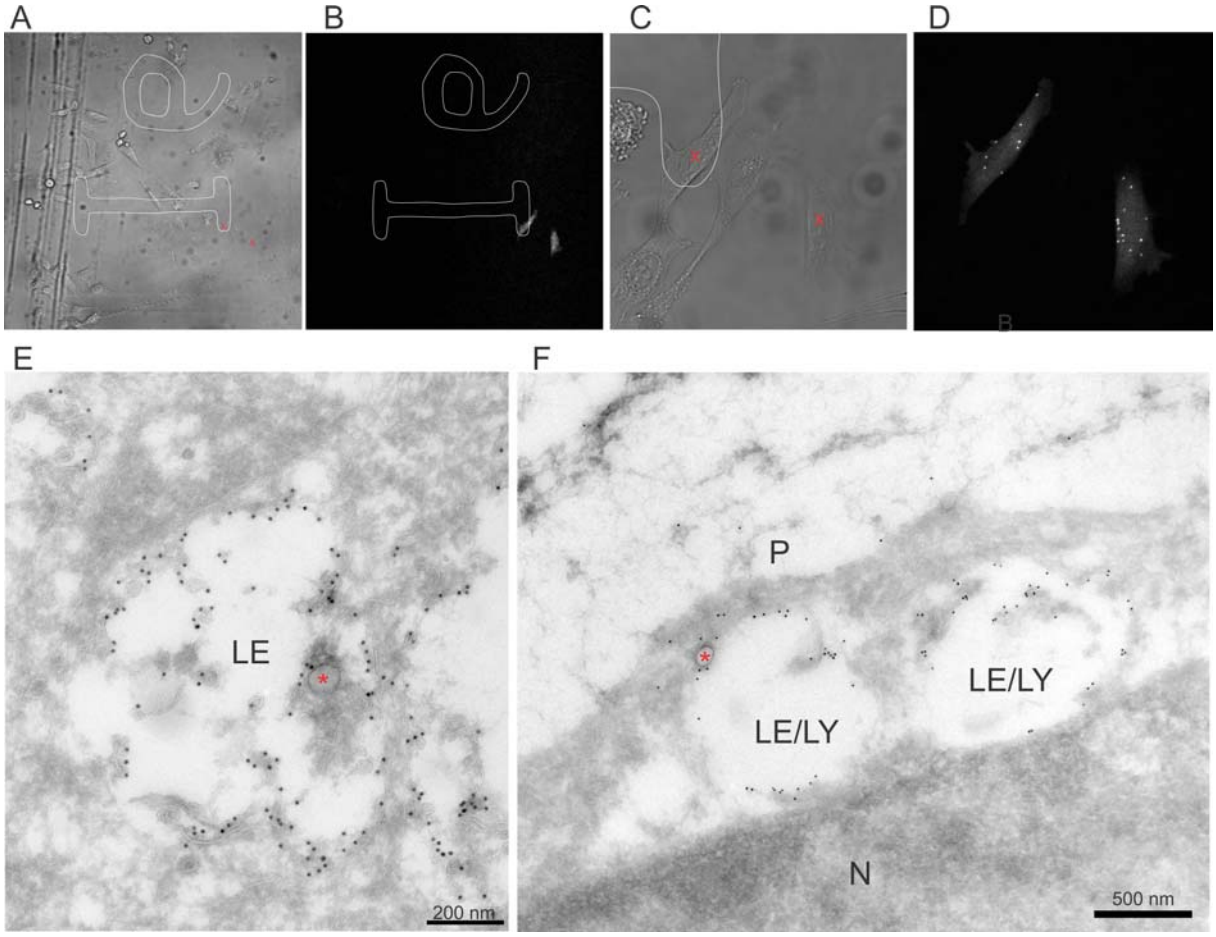

Fig 9. Electron Microscopy of HeLa cells immune gold-labeled for LAMP1 (10 nm gold particles, black dots), that were injected with 100 nm polystyrene beads. (A and C) show injected cells (2 injected cells indicated with red cross) on the gridded coverslip while (B and D) show the fluorescence of the injected cells. Cryosections of injected cells were viewed in detail with EM (E and F). Polystyrene beads are indicated with a red asterix. P: plasma membrane, N: nucleus, LE/LY: late endosome/lysosome. Cells were fixed and processed 24 hours after the initial administration of nanoparticles

DISCUSSION

In non-viral gene delivery, we aim to introduce plasmid DNA or messenger RNA into the target cells, to induce the expression of therapeutically relevant proteins. While pDNA needs to reach the nucleus of the cells, mRNA can be translated into the cytoplasm of the cells. As naked nucleic acids are not efficiently taken up in the cells, they are routinely complexed to cationic polymers or cationic liposomes. The resulting complexes are mostly taken up by endocytosis (28). Then, nanoparticles need to escape the endosomes to avoid degradation in the lysosomal compartment. Up to now, it is generally accepted that endosomal escape is a rare event, and could be the major bottleneck in the nucleic acid's delivery (29). It is also generally accepted that nanoparticles which gained access to the cytoplasm after endosomal escape, remain in the cytoplasm for a sufficient long time to lead to a therapeutic effect.

In this research paper, however, three independent observations demonstrate that nanoparticles that were directly delivered to the cytoplasm of the cells, can be captured in vesicles and are delivered to the degradative lysosomal compartment. First, SPT shows that nanoparticles which are freely present in the cytoplasm of the cells were completely immobile immediately after injection. This is confirmed by the alpha values, which give information about the mode of diffusion of nanoparticles. Brownian motion is characterized by an alpha value of 1. Alpha values less than 1 indicate restricted transport (slower than Brownian motion), while alpha values above 1 show directed transport (faster than Brownian motion). The distribution of alpha values immediately after injection demonstrates that about 90% of the nanoparticles have an alpha value lower than 0.4, indicating these particles are immobile in the cytoplasm. Upon overnight incubation, however, 55% of nanoparticles now display alpha values between 0.4 and 1, showing increased motion. 20% of nanoparticles even shows clear directed transport, with an alpha value above 1. This directed transport is typical for endocytic vesicles which use motor proteins to travel along the microtubules in the cytoplasm. It should be noted that also the particles with alpha values between 0.4 and 1 showed directed transport. If the particles, however, remain stationary for some part of the track, the average alpha value decreases below 1. As only 25% of nanoparticles remained completely stationary after overnight incubation, these

observations point out that about 75% of nanoparticles are transported inside vesicles, indicative for an autophagy response. In a next set of experiments, colocalization was performed between red labeled nanoparticles and green labeled lysosomes (GFP-LAMP1) or autophagosomes (GFP-LC3). Both type of nanoparticles colocalize with lysosomes and autophagosomes after overnight incubation, giving additional proof that nanoparticles are taken up by an autophagy response. Also here, colocalization analysis demonstrate that more than 75% of nanoparticles are eventually delivered to the lysosomes (Fig 6). Colocalization with autophagosomes is less, with respectively 30 ± 4 and 50 ± 9 of polystyrene beads and PEI/DNA nanoparticles taken up after overnight incubation. It should be noted, however that the GFP-LC3 signal is lost when the inner autophagosomal membrane degrades after lysosomal fusion. Therefore, it is possible that non-colocalized nanoparticles were already delivered to the lysosomal compartment. Alternatively, they are still freely present in the cytoplasm of the cells, which does however not agree with the increased mobility observed by SPT or the colocalization observed with GFP-LAMP1 positive vesicles. Finally, we performed electron microscopy (EM) to show that nanoparticles are present inside vesicles and not just bound to the surface of them. It should be noted that finding nanoparticles in EM was a rare event. Unlike confocal imaging or SPT, where the whole cell is imaged, cells for EM are cut into 65 nm thick cryosections. With the injection conditions used, the cells contain on average between 8-20 nanoparticles. We assume that the combination of cutting the cells in cryosections, together with the possible washing out of beads during subsequent washing and fixation steps could contribute to the fact that it was not straightforward to find beads in the injected cells samples.

The induction of autophagy upon directly introducing nanoparticles inside the cytoplasm is an important additional intracellular barrier that is so far not taken into account. For free plasmid DNA it has been suggested that autophagy can be induced when the pDNA is delivered to the cell's cytoplasm by microinjection (27). As autophagy is considered as an innate intracellular defense mechanism to clear the cells from incoming pathogens such as viruses and bacteria, it seems logic that also foreign DNA sequences could be recognized in the cytoplasm of the cells by the cellular DNA sensors. For pDNA/PEI complexes, parts of pDNA that are exposed at the surface of the complexes could trigger

autophagy in this way. This could also explain the stronger induction of autophagosomes upon endosomal uptake of pDNA/PEI nanoparticles as seen in Figure 5. For the inert polystyrene beads also used in this study, however, the trigger for autophagy is not clear yet. As the beads are charged, it could be that they bind with oppositely charged cellular proteins which act as the messenger molecules to induce autophagy. Alternatively, polystyrene beads could be non-specifically cleared from the cytoplasm during the capturing of defective cell organelles.

Very recently, Lisse et al demonstrated autophagy on injected ferritin light chain based nanoparticles of much smaller size (9-12 nm) then the nanoparticles used in this study (30). It thus seems that cytoplasmic recognition and clearance by autophagy is a general cellular defense mechanism against nanoparticles, even when they did not enter the cells through endocytosis. This in contrast to the observations by Roberts et al (17), who suggested that the autophagy machinery mainly recognizes the endosomes carrying these complexes, while cytoplasmic complexes were apparently resistant to further capture by autophagosomes. While it has been demonstrated that nanoparticles that enter the cells through endocytosis, can induce autophagy and that inhibiting this autophagy response increases the therapeutic effect (17) (31) (32), our paper adds to those data the direct demonstration of the uptake and presence of nanoparticles that entered the cytoplasm by electroporation or microinjection in autolysosomes. It should be noted that a large macromolecule such as TRITC-dextran used for co-injections does not colocalize with GFP-LC3 when injected on itself. When co-injected with nanoparticles, however, the TRITC-dextran is present in autophagosomes, indicating the co-capturing of this cytoplasmic molecule when autophagy is induced (Suppl. Fig. 2). This also demonstrates that the microinjection procedure on itself does not induce autophagy in the injected cells.

The possibility to capture cytoplasmic nanoparticles by an autophagy response sheds new light on the endosomal escape dogma. Up to now, it is accepted that endosomal escape is a rare event, with more than 90% of the delivered nanoparticles ending up in the degradative lysosomal compartment (33). Our observations, however, implicate that a single endosomal escape event does not guarantee that a nanoparticle remains in the cytoplasm for a sufficient long time to induce biological activity. Rather, the escaped nanoparticles can be re-captured by autophagy, again physically separating them from the

cytoplasm by a double-lipid membrane. This in turn implies that nanoparticles need one or more additional endosomal escape events to reach the cytoplasm and to escape from the lysosomes. The occurrence of autophagy could thus explain why most nanoparticles are seen within the endosomal compartment, even if efficient endosomal escape would occur. The average time before cytoplasmic nanoparticles or free nucleic acids are captured in autophagosomes remains to be elucidated. Also, which intracellular molecules trigger the recognition of nanoparticles and nucleic acids for autophagy remains an open question. It is becoming clear, however, that autophagy is an important barrier in non-viral gene delivery that should be taken into account, both for complexes entering the cells through endocytosis or freely present in the cytoplasm of the cells. The recognition of autophagy as an important barrier and the possibility to inhibit an autophagy response opens up new avenues in non-viral gene delivery.

CONCLUSION

Several intracellular barriers exist to non-viral gene delivery, including cellular uptake, endosomal escape, degradation of nucleic acids and delivery to the nucleus of the cells. Recently, the possibility of nanoparticles to induce the occurrence of autophagy has been suggested. This results in the accelerated delivery of the nanoparticles to the lysosomal compartment, leading to their degradation and hence limited therapeutic efficiency. This research paper demonstrates that the autophagy machinery can also recognize and capture nanoparticles that were directly delivered to the cytoplasm of the cells by microinjection or electroporation. This indicates that upon endosomal escape, cytoplasmic nanoparticles most likely can re-enter the endosomal vesicles, implying the need for additional endosomal escape events. This on its turn could contribute to the large fraction of administered nanoparticles that remain present in the endosomal compartment, preventing their biological activity. A better understanding of the triggers of autophagy and possible ways of interfering with the autophagy pathway could lead to an enhanced therapeutic effect for non-viral gene delivery.

ACKNOWLEDGMENTS

K. Remaut is a postdoctoral fellow of the Research Foundation Flanders. Their financial support is acknowledged with gratitude. Prof. Felix Randow is kindly acknowledged for the supply of HeLa-LC3 cells. This work is part of a EuroBioImaging concept study.

FIGURES

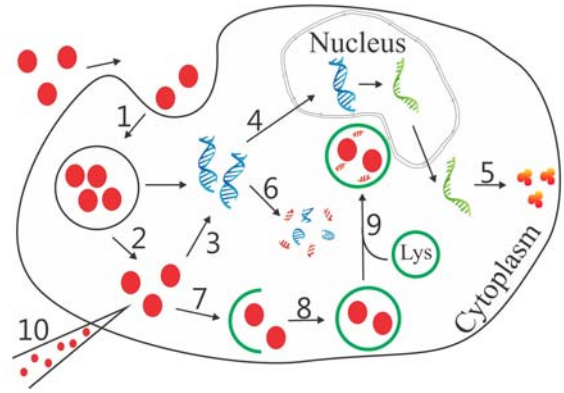

Fig1. Intracellular barriers to non-viral gene delivery. After cellular entry (1), nanoparticles have to escape from the endosomes (2) and release nucleic acids in the cytoplasm of the cells (3). Plasmid DNA then needs to travel to the nucleus (4), while mRNA can be translated to proteins in the cytoplasm of the cells (5). Clearly, degradation of nucleic acids should be avoided (6). When autophagy occurs, a phagophore isolates cytoplasmic material (7) and closes on itself to form an autophagosome (8). These fuse with lysosomes to form an autolysosome (9) in which the cytoplasmic cargo is degraded. In this research article, nanoparticles are directly delivered to the cytoplasm of the cells by microinjection (10).

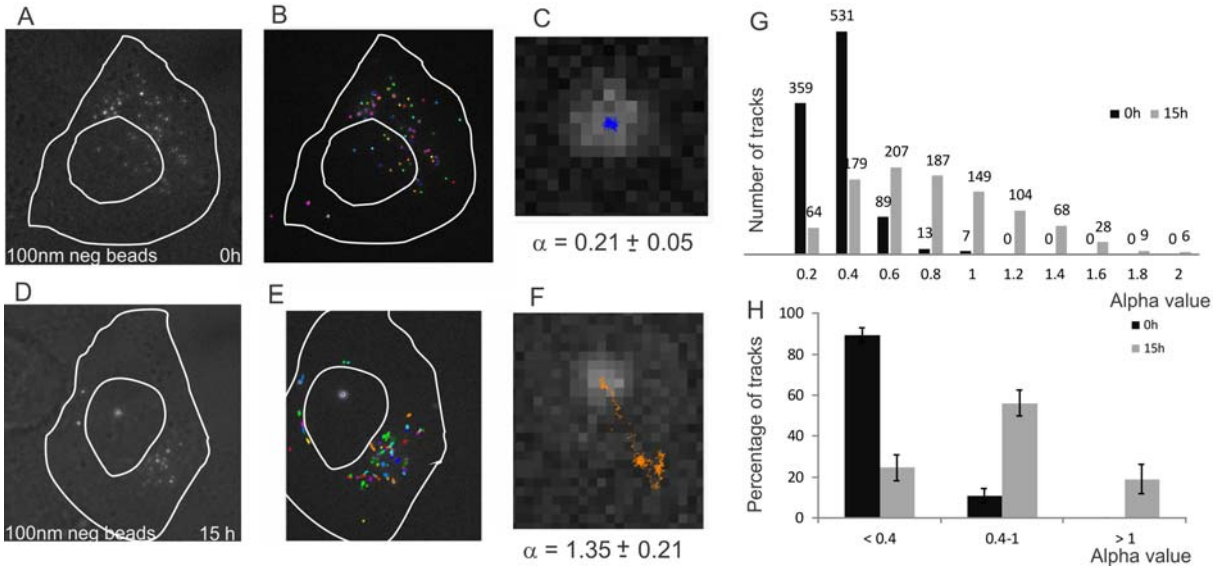

Fig2. Single particle tracking in HeLa cells injected with 100 nm negatively charged green polystyrene beads. (A and D) Transmission image immediately and 15 hours following injection, (B and E) tracks of polystyrene beads and (C and F) zoom in on a single track. The position of the cytoplasm and nucleus is demonstrated by white lines. (G) represents a histogram of the number of tracks with an alpha value as depicted in the x-axis. (H) shows the percentages of tracks with an alpha value as depicted in the x-axis. Black bars: immediately after injection . Grey bars: after overnight incubation. Representative videos can be viewed in supplementary information.

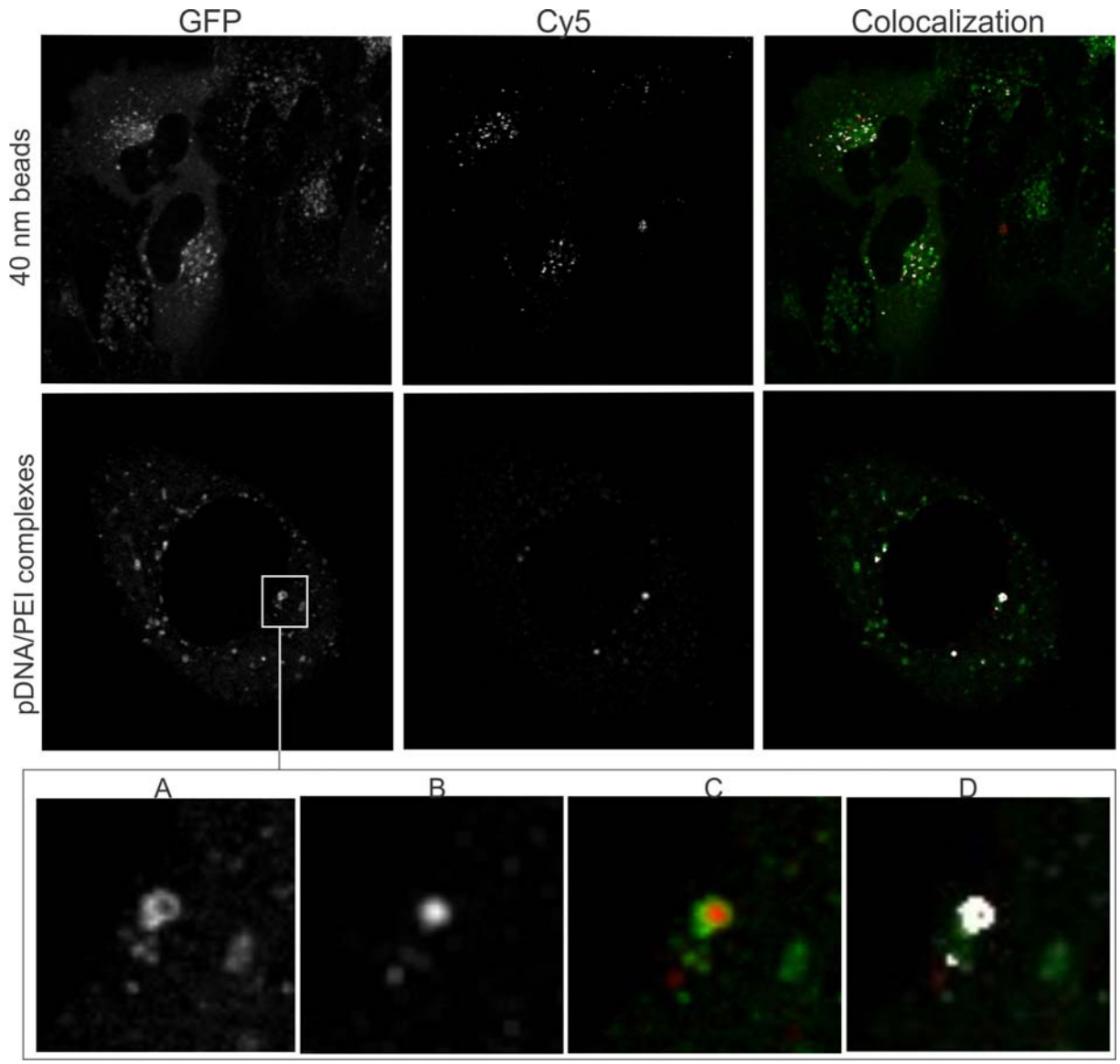

Fig 3. Confocal images of HeLa cells expressing GFP-LAMP1 (GFP), that were injected with red labeled polystyrene beads or pDNA/PEI nanoparticles (Cy5). Colocalization between green and red fluorescence is shown as white dots, while non-colocalized lysosomes or nanoparticles appear in green or red respectively (Colocalization). Insert shows a detail of a GFP-LAMP1 positive membrane (A, green channel) that surrounds a pDNA/PEI nanoparticle (B, red channel). C represent the overlay of A and B, while D depicts the colocalized pixels in white.

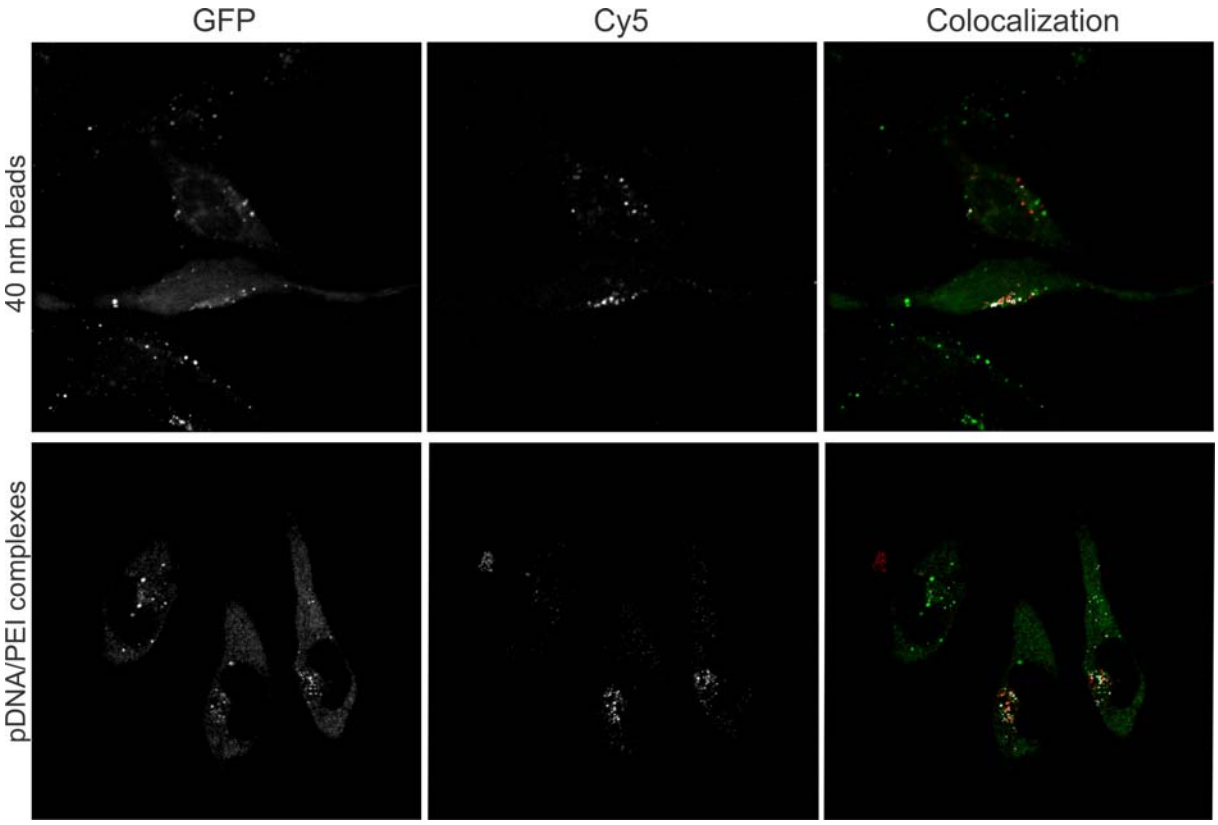

Fig 4. Confocal images of HeLa cells expressing GFP-LC3 (GFP), that were injected with red labeled polystyrene beads or pDNA/PEI nanoparticles (Cy5). Colocalization between green and red fluorescence is shown as white dots, while non-colocalized autophagosomes or nanoparticles appear in green or red respectively (Colocalization).

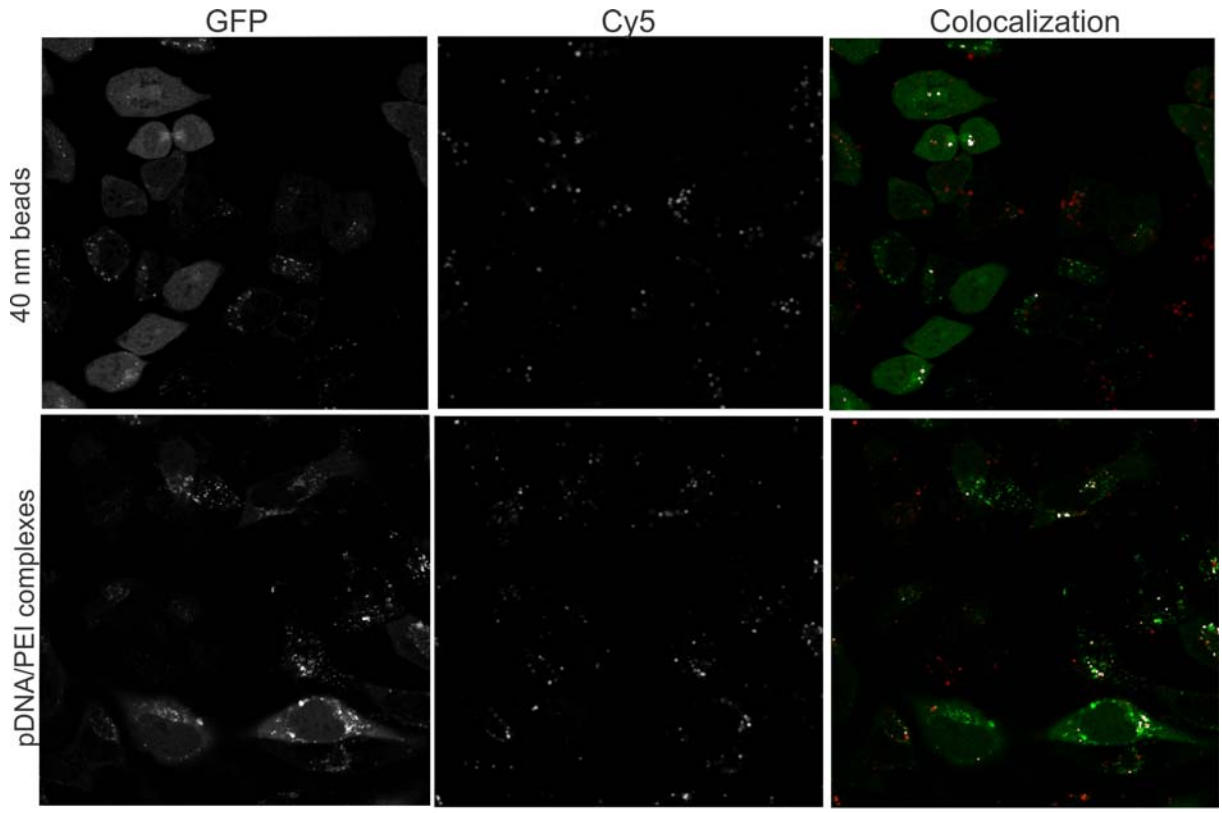

Fig 5. Confocal images of HeLa cells expressing GFP-LC3 (GFP), that were incubated with red labeled polystyrene beads or pDNA/PEI nanoparticles (Cy5). Colocalization between green and red fluorescence is shown as white dots, while non-colocalized autophagosomes or nanoparticles appear in green or red respectively (Colocalization).

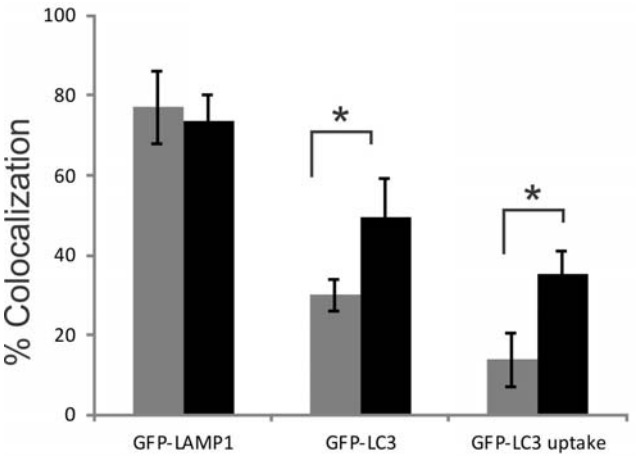

Fig 6. Percentage of colocalization between red polystyrene beads (grey bars) and red PEI/DNA nanoparticles (black bars) with green labeled GFP-LAMP1 or GFP-LC3 vesicles as depicted in the x-axis. (GFP-LC3 uptake) shows colocalization when nanoparticles were taken up by endocytosis. Significant differences between polystyrene beads and PEI/DNA nanoparticles were determined by a student t-test. * denotes a P value < 0.05.

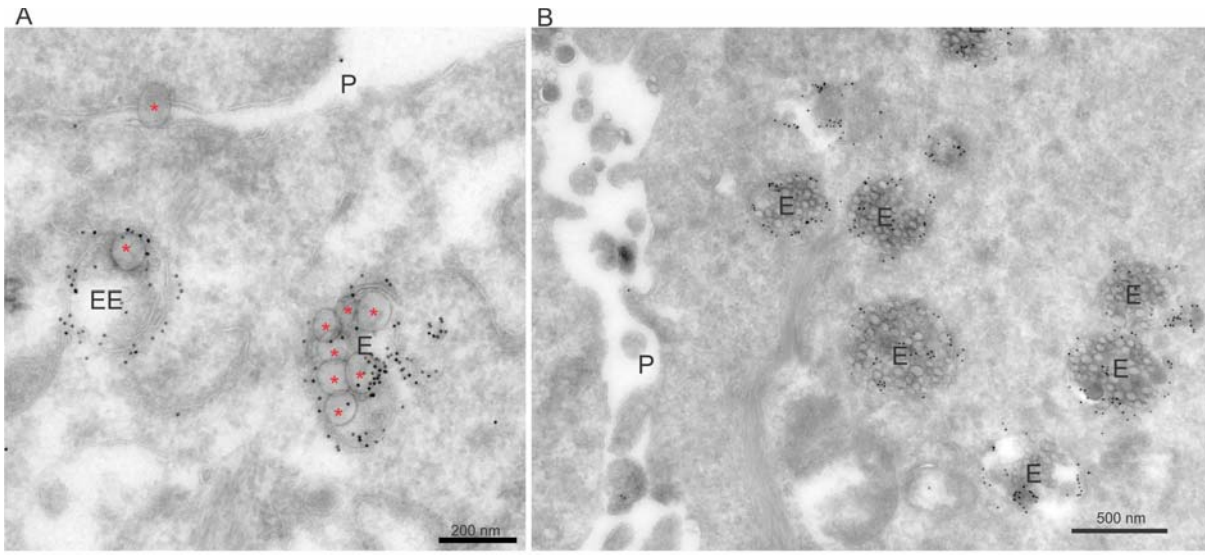

Fig 7. Electron Microscopy of HeLa cells immune gold-labeled for LAMP1 (10 nm gold particles, black dots), that were incubated with 100 nm (A) or 40 nm (B) polystyrene beads. Polystyrene beads (indicated with red asterix in A) are clearly visible in the endosomal lumen. P: plasmamembrane, EE: early endosome, E: later stage endosomes. Cells were fixed and processed 24 hours after the initial administration of nanoparticles.

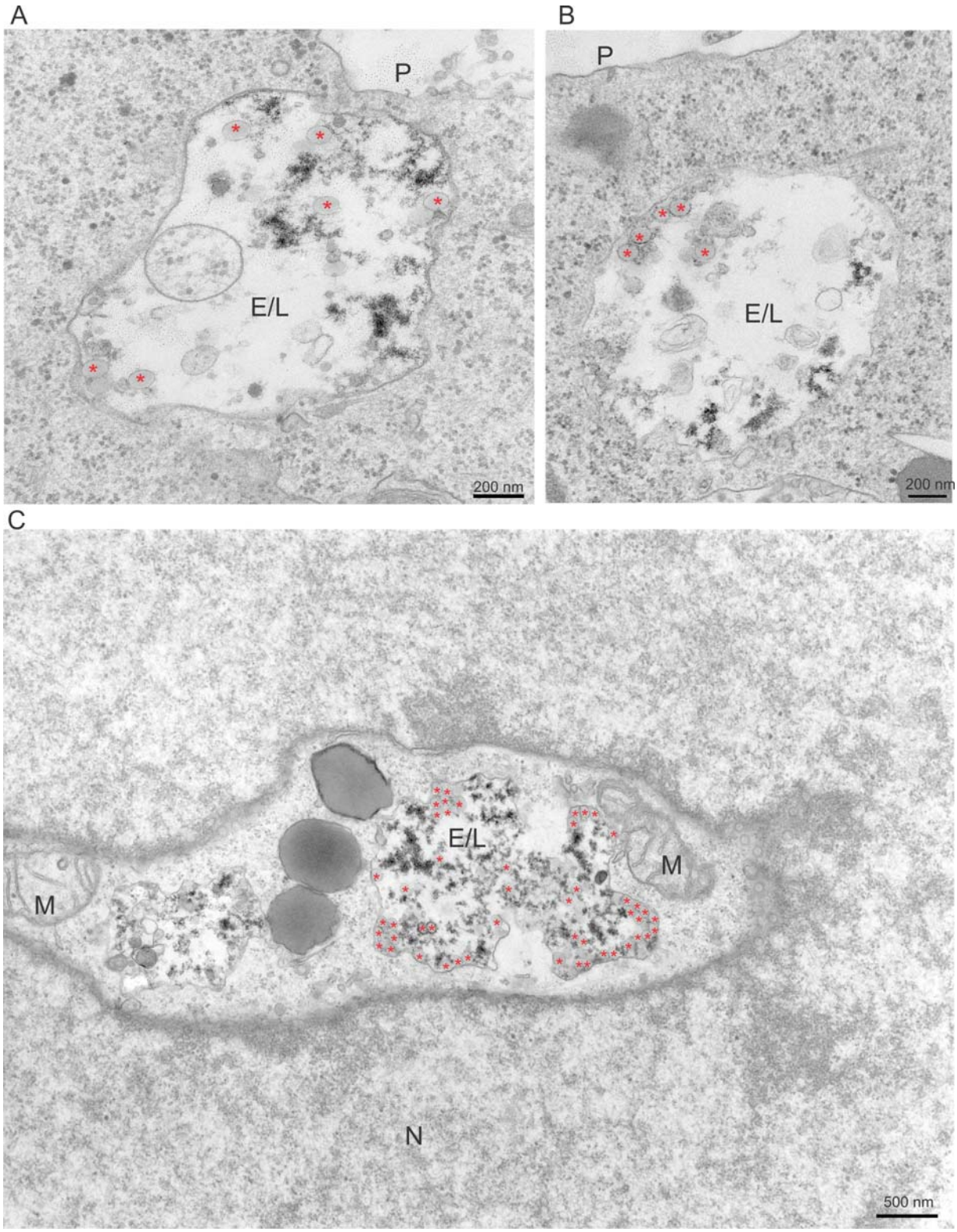

Fig 8. Electron Microscopy of HeLa cells that were electroporated with 100 nm polystyrene beads. Polystyrene beads are indicated with a red asterix. P: plasma membrane, N: nucleus, E/L: endosome/lysosome, M: mitochondrion. Cells were fixed and processed 24 hours after the initial administration of nanoparticles. (A, B and C) represent 3 different cells.

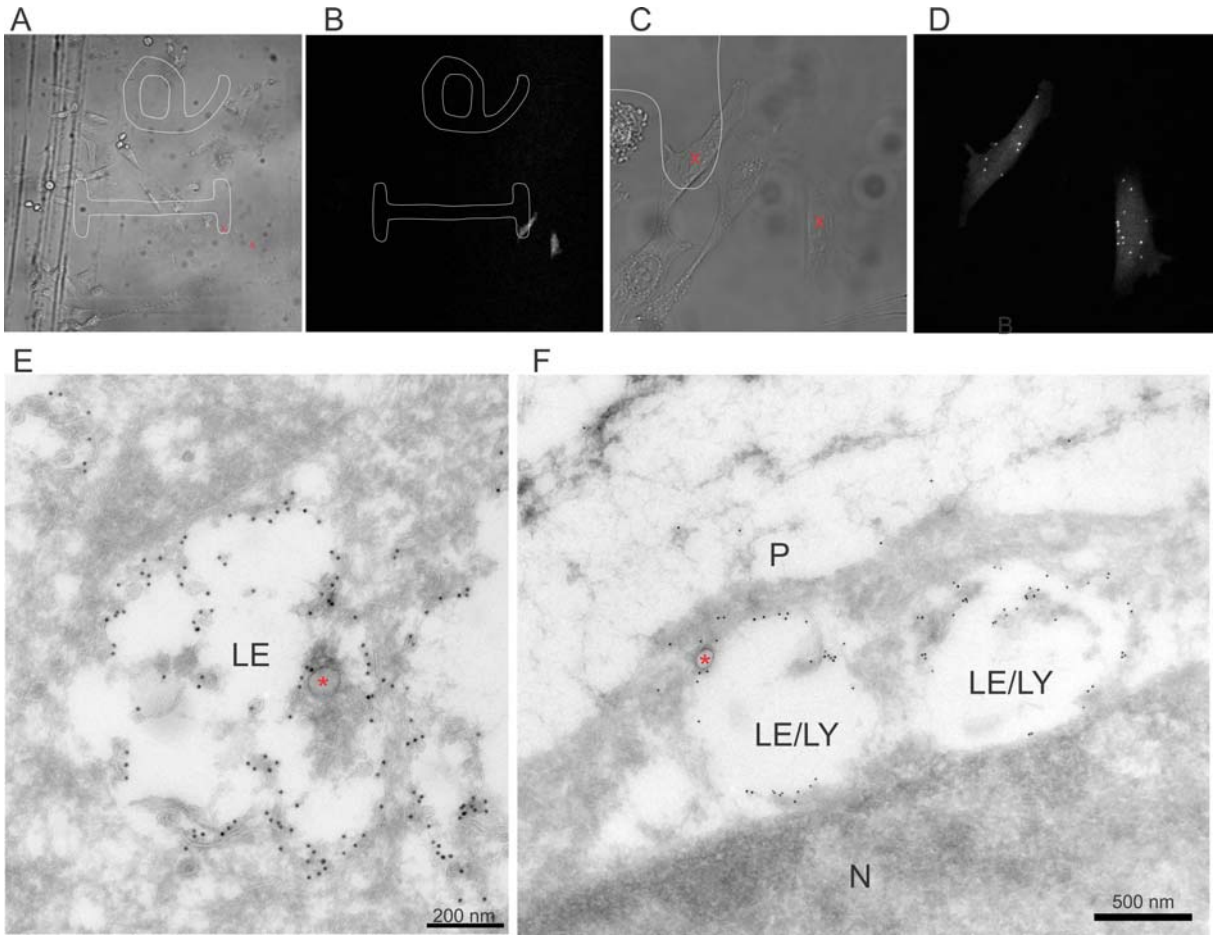

Fig 9. Electron Microscopy of HeLa cells immune gold-labeled for LAMP1 (10 nm gold particles, black dots), that were injected with 100 nm polystyrene beads. (A and C) show injected cells (2 injected cells indicated with red cross) on the gridded coverslip while (B and D) show the fluorescence of the injected cells. Cryosections of injected cells were viewed in detail with EM (E and F). Polystyrene beads are indicated with a red asterix. P: plasma membrane, N: nucleus, LE/LY: late endosome/lysosome. Cells were fixed and processed 24 hours after the initial administration of nanoparticles

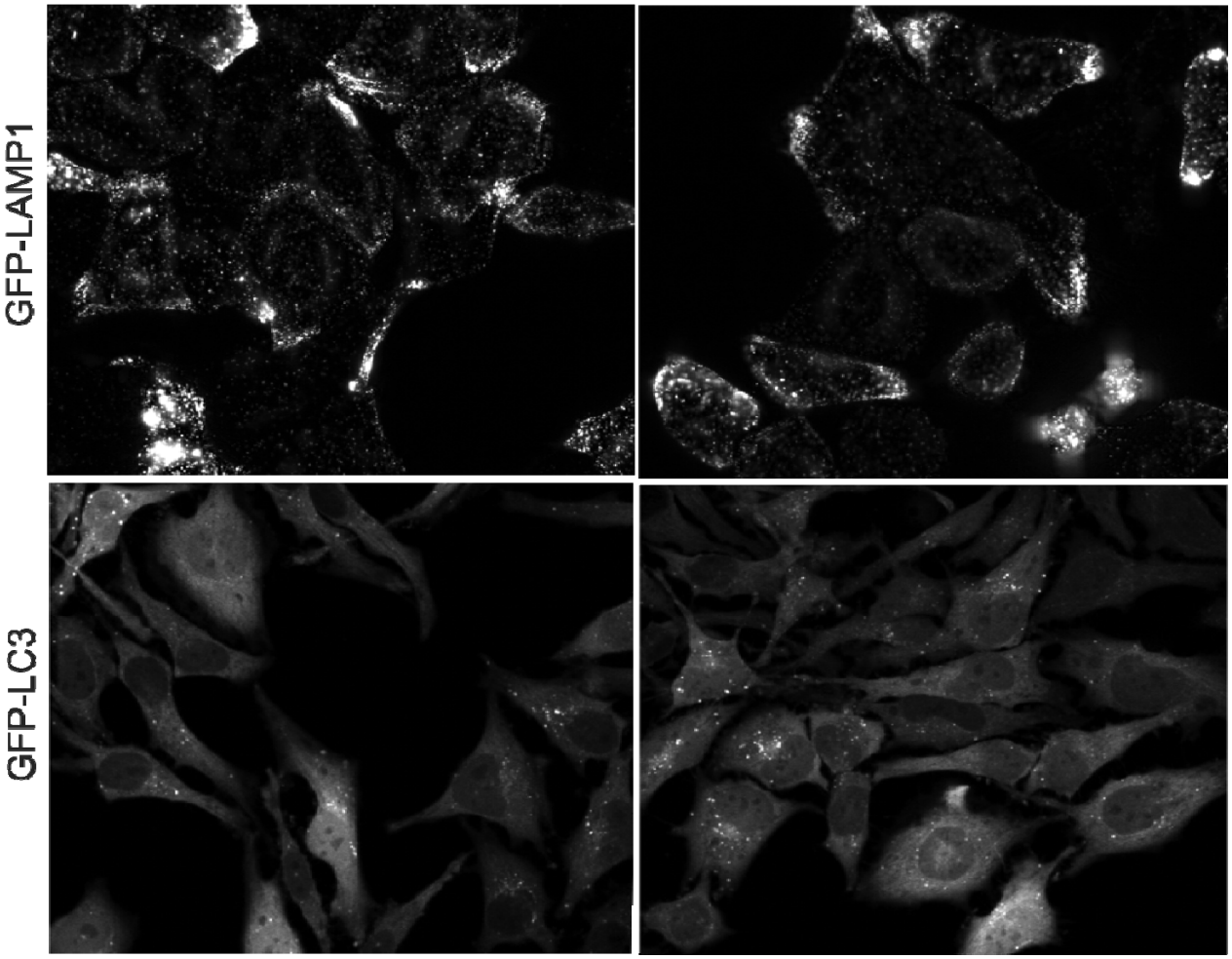

Suppl. Fig 1. Expression levels of GFP-LAMP1 (top row) and GFP-LC3 (bottom row) in non-treated HeLa cells.

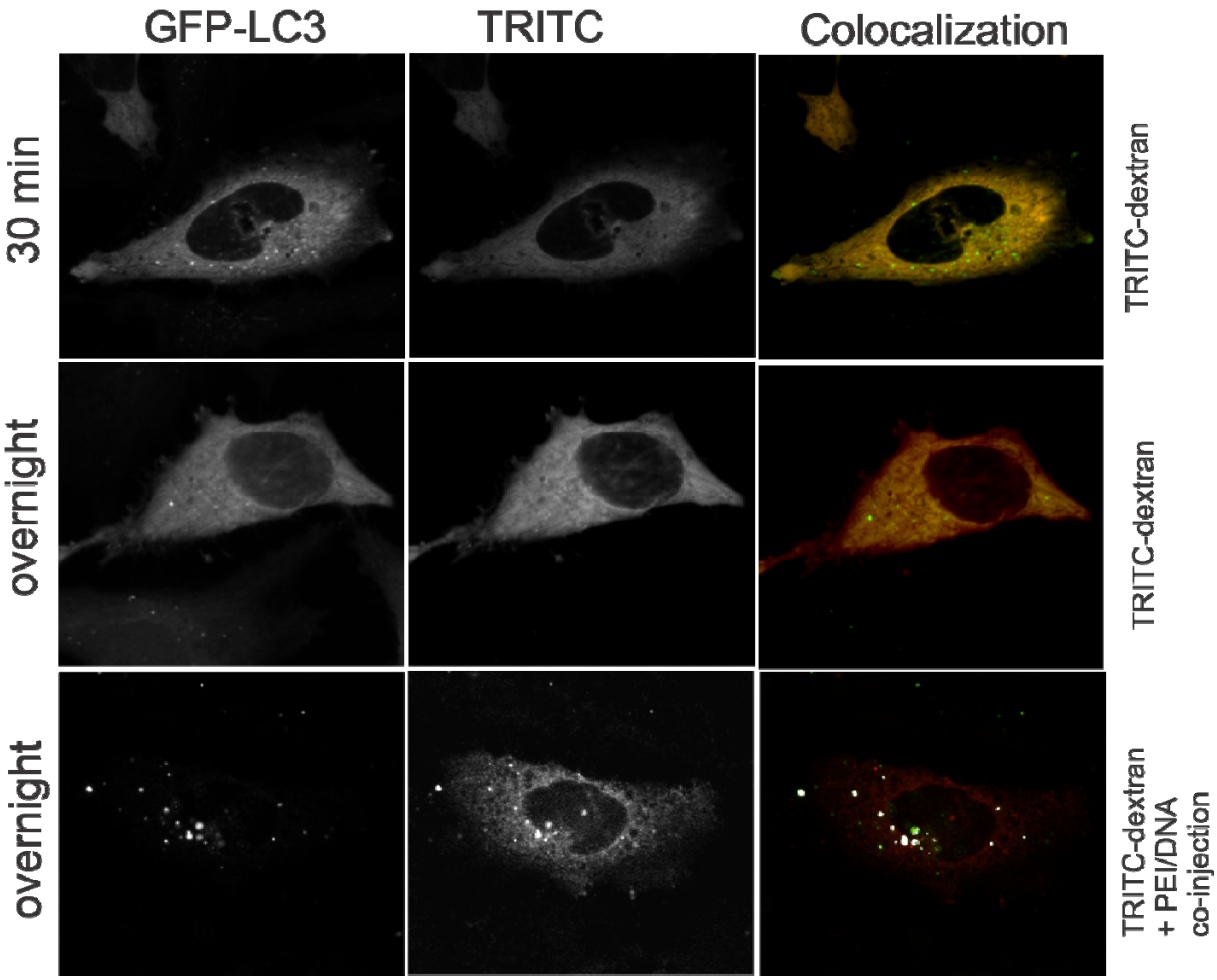

Suppl Fig 2. Colocalization between GFP-LC3 autophagosomes and 70 kDa TRITC-dextran. When injected as such, TRITC-dextran homogenously spreads in the cytoplasm immediately after injection and only occasionally colocalizes with GFP-LC3 vesicles after overnight incubation. In the presence of PEI/DNA nanoparticles, however, TRITC-dextran seems to be co-captured in autophagosomes.

Reference List

1. Remaut,K., Sanders,N.N., De Geest,B.G., Braeckmans,K., Demeester,J. and De Smedt,S.C. (2007) Nucleic acid delivery: where material sciences and bio-sciences meet. *Materials Science & Engineering Reports*, **58**, 117-161.

2. Scholz,C. and Wagner,E. (2012) Therapeutic plasmid DNA versus siRNA delivery: common and different tasks for synthetic carriers. *J. Control Release*, **161**, 554-565.

3. Samal,S.K., Dash,M., Van,V.S., Kaplan,D.L., Chiellini,E., van,B.C., Moroni,L. and Dubruel,P. (2012) Cationic polymers and their therapeutic potential. *Chem. Soc. Rev.*, **41**, 7147-7194.

4. Braeckmans,K., Buyens,K., Naeye,B., Vercauteren,D., Deschout,H., Raemdonck,K., Remaut,K., Sanders,N.N., Demeester,J. and De Smedt,S.C. (2010) Advanced fluorescence microscopy methods illuminate the transfection pathway of nucleic acid nanoparticles. *J. Control Release*, **148**, 69-74.

5. Raemdonck,K., Vandenbroucke,R.E., Demeester,J., Sanders,N.N. and De Smedt,S.C. (2008) Maintaining the silence: reflections on long-term RNAi. *Drug Discov. Today*, **13**, 917-931.

6. Li,D.S. and Huang,L. (2006) Gene therapy progress and prospects: non-viral gene therapy by systemic delivery. *Gene Ther.*, **13**, 1313-1319.

7. Pack,D.W., Hoffman,A.S., Pun,S. and Stayton,P.S. (2005) Design and development of polymers for gene delivery. *Nat. Rev. Drug Discov.*, **4**, 581-593.

8. Jhaveri,A.M. and Torchilin,V.P. (2014) Multifunctional polymeric micelles for delivery of drugs and siRNA. *Front Pharmacol.*, **5**, 77.

9. Deshpande,P.P., Biswas,S. and Torchilin,V.P. (2013) Current trends in the use of liposomes for tumor targeting. *Nanomedicine. (Lond)*, **8**, 1509-1528.

10. Frohlich,E. (2012) The role of surface charge in cellular uptake and cytotoxicity of medical nanoparticles. *Int. J. Nanomedicine.*, **7**, 5577-5591.

11. Rejman,J., Conese,M. and Hoekstra,D. (2006) Gene transfer by means of lipo- and polyplexes: Role of clathrin and caveolae-mediated endocytosis. *J. Liposome Res.*, **16**, 237-247.

12. Rejman,J., Oberle,V., Zuhorn,I.S. and Hoekstra,D. (2004) Size-dependent internalization of particles via the pathways of clathrin-and caveolae-mediated endocytosis. *Biochem. J.*, **377**, 159-169.

13. Hyvonen,Z., Hamalainen,V., Ruponen,M., Lucas,B., Rejman,J., Vercauteren,D., Demeester,J., De,S.S. and Braeckmans,K. (2012) Elucidating the pre- and post-nuclear intracellular processing of 1,4-dihydropyridine based gene delivery carriers. *J. Control Release*, **162**, 167-175.

14. Vercauteren,D., Piest,M., van der Aa,L.J., Al,S.M., Jones,A.T., Engbersen,J.F., De Smedt,S.C. and Braeckmans,K. (2011) Flotillin-dependent endocytosis and a phagocytosis-like mechanism for cellular internalization of disulfide-based poly(amido amine)/DNA polyplexes. *Biomaterials*, **32**, 3072-3084.

15. Symens,N., Walczak,R., Demeester,J., Mattaj,I., De Smedt,S.C. and Remaut,K. (2011) Nuclear inclusion of nontargeted and chromatin-targeted polystyrene beads and plasmid DNA containing nanoparticles. *Mol. Pharm.*, **8**, 1757-1766.

16. Mehrpour,M., Esclatine,A., Beau,I. and Codogno,P. (2010) Overview of macroautophagy regulation in mammalian cells. *Cell Res.*, **20**, 748-762.

17. Roberts,R., Al-Jamal,W.T., Whelband,M., Thomas,P., Jefferson,M., van den Bossche,J., Powell,P.P., Kostarelos,K. and Wileman,T. (2013) Autophagy and formation of tubulovesicular autophagosomes provide a barrier against nonviral gene delivery. *Autophagy.*, **9**, 667-682.

18. Martens,T.F., Vercauteren,D., Forier,K., Deschout,H., Remaut,K., Paesen,R., Ameloot,M., Engbersen,J.F., Demeester,J., De Smedt,S.C. *et al.* (2013) Measuring the intravitreal mobility of nanomedicines with single-particle tracking microscopy. *Nanomedicine. (Lond)*, **8**, 1955-1968.

19. Rombouts,K., Martens,T.F., Zagato,E., Demeester,J., De Smedt,S.C., Braeckmans,K. and Remaut,K. (2014) Effect of Covalent Fluorescence Labeling of Plasmid DNA on Its Intracellular Processing and Transfection with Lipid-Based Carriers. *Mol. Pharm.*, **11**, 1359-1368.

20. Frohlich,E., Meindl,C., Roblegg,E., Ebner,B., Absenger,M. and Pieber,T.R. (2012) Action of polystyrene nanoparticles of different sizes on lysosomal function and integrity. *Part Fibre. Toxicol.*, **9**, 26.

21. van Rijnsoever,C., Oorschot,V. and Klumperman,J. (2008) Correlative light-electron microscopy (CLEM) combining live-cell imaging and immunolabeling of ultrathin cryosections. *Nat. Methods*, **5**, 973-980.

22. Slot,J.W. and Geuze,H.J. (2007) Cryosectioning and immunolabeling. *Nat. Protoc.*, **2**, 2480-2491.

23. Vicidomini,G., Gagliani,M.C., Canfora,M., Cortese,K., Frosi,F., Santangelo,C., Di Fiore,P.P., Boccacci,P., Diaspro,A. and Tacchetti,C. (2008) High data output and automated 3D correlative light-electron microscopy method. *Traffic.*, **9**, 1828-1838.

24. Klumperman,J. and Raposo,G. (2014) The Complex Ultrastructure of the Endolysosomal System. *Cold Spring Harb. Perspect. Biol.*.

25. Bolte,S. and Cordelieres,F.P. (2006) A guided tour into subcellular colocalization analysis in light microscopy. *J. Microsc.*, **224**, 213-232.

26. Klionsky,D.J. and et al. (2012) guidelines for the use and interpretation of assays monitoring autophagy. *Autophagy*, **8**, 445-544.

27. Watson,R.O., Manzanillo,P.S. and Cox,J.S. (2012) Extracellular M. tuberculosis DNA targets bacteria for autophagy by activating the host DNA-sensing pathway. *Cell*, **150**, 803-815.

28. Vercauteren,D., Rejman,J., Martens,T.F., Demeester,J., De Smedt,S.C. and Braeckmans,K. (2012) On the cellular processing of non-viral nanomedicines for nucleic acid delivery: mechanisms and methods. *J. Control Release*, **161**, 566-581.

29. Martens,T., Remaut,K., Demeester,J., De Smedt,S.C. and Braeckmans,K. (2014) Intracellular delivery of nanomaterials: how to catch endosomal escape in the act. *Nano Today*, **in press**.

30. Lisse,D., Richter,C.P., Drees,C., Birkholz,O., You,C., Rampazzo,E. and Piehler,J. (2014) Monofunctional stealth nanoparticle for unbiased single molecule tracking inside living cells. *Nano Lett.*, **14**, 2189-2195.

31. Zhang,X., Dong,Y., Zeng,X., Liang,X., Li,X., Tao,W., Chen,H., Jiang,Y., Mei,L. and Feng,S.S. (2014) The effect of autophagy inhibitors on drug delivery using biodegradable polymer nanoparticles in cancer treatment. *Biomaterials*, **35**, 1932-1943.

32. Kobayashi,S., Kojidani,T., Osakada,H., Yamamoto,A., Yoshimori,T., Hiraoka,Y. and Haraguchi,T. (2010) Artificial induction of autophagy around polystyrene beads in nonphagocytic cells. *Autophagy*, **6**, 36-45.

33. Vercauteren,D., Deschout,H., Remaut,K., Engbersen,J.F., Jones,A.T., Demeester,J., De Smedt,S.C. and Braeckmans,K. (2011) Dynamic colocalization microscopy to characterize intracellular trafficking of nanomedicines. *ACS Nano.*, **5**, 7874-7884.